 doi.org/10.1002/mawe.202000300

Single-wall carbon nanotubes-chitosan nanocomposites: Surface wettability, mechanical and thermal properties

Einwand-Kohlenstoffnanoröhren-Chitosan-Nanokomposite: Benetzbarkeit der Oberflächen, mechanische und thermodynamische Eigenschaften

M.Á.V. Rodrigues[1], M.M. Horn[2], V.C.A. Martins[1], A.M.G. Plepis[1, 3]

Functionalized single-wall carbon nanotubes (*f*-SWCN) are dispersed in chitosan films by self-assembly of both components in aqueous media. This carbon form is a promising nanofiller to achieve nanocomposites with refined thermal, mechanical and surface features. In this study, we investigated the influence of functionalized single-wall carbon nanotubes concentration on the resulting properties of the nanocomposites structures. Functionalized single-wall carbon nanotubes are dispersed on a molecular scale in the polymeric matrix due to electrostatic interactions between both components. The thermal and mechanical properties have been characterized by thermogravimetric analysis and dynamic mechanical analysis, respectively, while their wettability is studied by water contact angle measurements. Mechanical resistance of the films is improved up to 18 % with the addition of functionalized single-wall carbon nanotubes, but the thermal stability is expressively reduced. A decrease in the surface hydrophobicity of 25 % is obtained after the inclusion of the nanofiller.

Keywords: Chitosan **/** carbon nanotubes **/** nanocomposites **/** nanofiller **/** films

Funktionalisierte Einwand-Kohlenstoffnanoröhren (f-SCWN) bilden mit Chitosan-Filmen eine Dispersion in wässrigen Lösungen. Diese Form des Kohlenstoffs ist ein vielversprechender Kandidat für Nanokomposite mit verbesserten Oberflächen-, thermodynamischen und mechanischen Eigenschaften. In dieser Studie wurde der Einfluss der funktionalisierten Einwand-Kohlenstoffnanoröhren-Konzentrationen auf die resultierenden Eigenschaften der Nanokomposit-Strukturen untersucht. Aufgrund der elektrostatischen Kräfte zwischen dem Chitosan-Film und den funktionalisierten Einwand-Kohlenstoffnanoröhren werden letztere in der Polymer-Matrix auf dem molekularen Level gelöst. Die resultierenden thermischen und mechanischen Eigenschaften wurden mittels thermogravimetrischer und dynami-

[1] Universidade de São Paulo, Instituto de Química de São Carlos, Av. Trabalhador Sãocarlense, 400, 13566-970, SÃO CARLOS, BRAZIL
[2] Universität Kassel, Physikalische Chemie der Nanomaterialien, Heinrich-Plett-Straße 40, 34132, KASSEL, GERMANY
[3] Universidade de São Paulo, Programa de Pós-graduação Interunidades Bioengenharia, Av. Trabalhador Sãocarlense, 400, 13566-970, SÃO CARLOS, BRAZIL

Corresponding author: M.M. Horn, Universität Kassel, Physikalische Chemie der Nanomaterialien, Heinrich-Plett-Straße 40, 34132, KASSEL, GERMANY,
E-Mail: mhorn@uni-kassel.de

Correction added on 23 August 2021, after first online publication: Projekt Deal funding statement has been added.

scher mechanischer Analysen untersucht, wohingegen die Benetzbarkeit der Oberfläche mit Kontaktwinkel-Untersuchungen ermittelt wurde. Der mechanische Widerstand der Filme wird durch Zugabe von funktionalisierten Einwand-Kohlenstoffnanoröhren um bis zu 18 % verbessert, die thermische Stabilität wird jedoch stark verringert. Nach dem Einschluss des Nanofüllstoffes wird eine Abnahme der Oberflächenhydrophobie von 25 % beobachtet.

Schlüsselwörter: Chitosan **/** Kohlenstoffnanoröhren **/** Nanokomposit **/** Nanofüllstoff **/** Filme

1 Introduction

The use of biopolymers has attracted significant interest in the development of composite films as they are derived from renewable sources including carbohydrates and proteins of plant or animal origin [1]. Chitosan is one of the most interesting biopolymers obtained from natural sources. Some prominent properties of chitosan are antibacterial and antifungal activity, non-toxicity, biocompatibility, biodegradability and solubility in acidic aqueous solutions. The solubility in acid media contributes to its processability into different forms, like scaffolds, gels, nanofibers, nanoparticles or films, which enables a wide range of applications [2, 3]. Chitosan is normally processed in gels and films and since the last decade, studies concerning the use of this biopolymer in the development of nanocomposites materials has been increased and equating in number to those traditional materials [4, 5].

The excellent film-forming property of chitosan allows the production of films using the solvent evaporation method. However, the resulting films are brittle with moderated mechanical properties [6, 7]. Many strategies were explored to improve the surface and mechanical properties of chitosan-based films, such as crosslink of chitosan chains or the association with materials like calcium phosphate cement, hydroxyapatite, clays or others to produce composites films [1, 3].

Bionanocomposites have been proposed as an alternative for conventional technologies to improve the mechanical and surface properties of biopolymers-based materials, but also to outperform other polymer intrinsic limitations, as water content or gas permeability. They are hybrid materials composed of a polymeric matrix reinforced with fillers which are in a nanometer range, as nanoparticles, nanosheets or carbon or halloysite nanotubes [4, 8, 9]. These nanofillers are usually added in small concentrations, up to 5 % in relation to the polymer, since the large aspect ratio of these structures allows multiple interactions with the matrix [5]. The main requirement is to produce a homogeneous dispersion of the nanofillers to achieve the maximal enhancement in the properties of the biopolymer films [10].

Among the various nanofillers employed, carbon nanotubes (CN) are some of those whose use has further increased in recent years. Carbon nanotubes presents a cylindrical structure formed by the winding of graphene sheets in tubes with nanometers in diameter and has been proposed to improve not only mechanical but also electrical, antimicrobial and thermal properties of polymeric matrices. When formed by a single-cylinder, carbon nanotube is called a single-walled carbon nanotube (SWCN) [6, 11, 12].

To prevent agglomerations and allow a good dispersion of carbon nanotubes within the polymeric matrix the electrostatic complexation can be considered. The improvement in the mechanical properties can be achieved by dispersion on a molecular scale due to the strong intermolecular forces between the components. To reach these interactions the use of functionalized carbon nanotubes is essential to allow the interfacial bonding between the carbon nanotubes and the polymeric matrix [13].

The reinforcement effect of carbon nanotubes must be maximized by a good dispersion without aggregation in the polymeric matrix. The use of ultrasound and/or high-speed stirring are the most convenient and easy methods to improve the dispersion of nanofillers. In addition, the surface of carbon nanotubes can be chemically modified to achieve a good dispersion by the insertion of active

chemical groups compatible with the polymeric matrix. Functionalized single-walled carbon nanotubes (*f*-SWCN) with hydrophilic carboxylic groups can interact with protonated amino groups of chitosan chains leading to good dispersion of the nanofillers at the nanoscale level, preventing the tendency of agglomeration. The hydrogen bond interaction between COOH and NH_2 groups at the atomic level was demonstrated by molecular dynamics simulation [14].

Polymeric nanocomposites produced by chitosan (CHI) and carbon nanotubes combine properties of its components to obtain new characteristics that are arduous to achieve individually [2]. Some studies reported the enhancement of mechanical properties of chitosan films by the addition of multi-walled carbon nanotubes (MWCN) showing that this nanofiller can be homogeneously dispersed in the chitosan matrix [6, 7, 15]. Changes in the properties depend not only on the compatibility of components but also on their concentration, the method used to prepare the nanocomposites and the conditions defined for this method (pH and relative humidity, for example) [4]. In this study, the self-assembly of both components in aqueous media was chosen to obtain the nanocomposite films. In addition, the concentration effect of functionalized single-walled carbon nanotubes on the surface wettability, mechanical, structural and thermal properties of chitosan films were investigated.

2 Experimental

2.1 Materials

Chitosan was obtained in our laboratory following an earlier described process, which includes demineralization, deacetylation and deproteinization of squid pens [16]. The average molecular weight (400 kDa) and the degree of acetylation (9 %) were determined by viscometry and conductometric titration, respectively, as previously described [17, 18]. Single-walled carbon nanotubes (SWCN), carboxylic acid functionalized was purchased in Sigma Aldrich.

2.2 Preparation of films

A 1 % chitosan solution was prepared by dissolution in acetic acid (1 %, v/v). After that, 0.10 mg, 0.25 mg or 0.50 mg of functionalized single-walled carbon nanotubes were added in 10 g of chitosan solution. Sonication and a mechanical homogenizer were employed to guarantee a proper nanofiller dispersion. The nanocomposite mixtures were poured in teflon molds (11 × 1 cm) and dried in air flux by solvent evaporation technique until thin films were easily removed from their supports. Films were labeled as CHCN10, CHCN25 and CHCN50 regarding the functionalized single-walled carbon nanotube concentration. A control chitosan film (CHI) was prepared following the same procedure. Films were stored in a humidity-controlled chamber (65 %).

2.3 Characterization of films

Films thickness was measured using a micrometer (Model M110-25, Mitutoyo MFG. Co. Ltd., Japan). Thickness measurements were taken at 10 different points along with the film and the mean values were calculated and used for mechanical measurements.

Scanning electronic microscopy (SEM) was carried out using a ZEISS LEO-440 microscope (Cambridge, England) with an OXFORD (model 7060) LEO 440 detector and an accelerating voltage of 20 keV. Samples with 1 cm × 1 cm were coated with a 6 nm gold layer.

Contact angle values were measured using a CAM 200 equipment (KSV Instruments – Helsinki, Finland). 3 µL of deionized water was dropped onto the surface of the films and the acquisition images were taken after 30 s to allow drop equilibration. The reported value represents the mean value of at least five independent measurements.

Fourier-transform infrared spectroscopy (FTIR) analysis of nanocomposites was performed in films produced by casting of its diluted solutions. functionalized single-walled carbon nanotubes spectrum was obtained by KBr pellet. Spectra were obtained using a Shimadzu IR Affinity-1 equipment at 4000 cm^{-1}–400 cm^{-1} interval with 4 cm^{-1} resolution.

Thermogravimetry (TG) analyzer Q50 (TA Instruments, USA) was employed to measure the weight loss of films under heating. Samples (10 mg) were heated in an alumina crucible between 25 °C and 800 °C at 10 °C min^{-1} in a synthetic air atmosphere (90 mL min^{-1}). The extrapolated onset temperature (T_{onset}) was determined with the software TA Universal Analysis.

Mechanical properties were measured at 25 °C in a dynamic mechanical analyzer Q800 (TA Instruments, USA) operating with the tension clamp using a force rate of 1 N min^{-1} and a distance between clamps of 10 mm. For each sample, at least 3 strips (6.3 mm × 15 mm) were tested and the tensile strength and the elongation at break were determined, respectively, as the point of maximum stress on the curve and the strain when the film ruptures.

Differences in thickness and mechanical properties of the films were analyzed using analysis of variance (ANOVA) followed by Tukey's test. The significance level was set at 5 %.

3 Results and discussion

The combination of nanodimension, electronic structure and chemical composition of carbon nanotubes results in superior electrical, mechanical and thermal properties of its nanocomposites. Even though be a versatile nanofiller the dispersibility in aqueous solvents is a limitation to explore its use. Chemical functionalization of the carbon nanotubes surface is a very effective technique that improves dispersibility in the polymeric matrix. In order to maximize the effects of carbon nanotubes and disperse it in a polymeric matrix, we used carboxylic functionalized single-walled carbon nanotubes to access the electrostatic interaction with chitosan chains. In addition, it was observed that stirring and sonication processes are necessary to disperse functionalized single-walled carbon nanotubes in the polymeric matrix and to obtain homogeneous solutions.

The final film-forming solutions were homogeneous which was observed even after some days, without any precipitate or agglomerate. Furthermore, in the solutions with a higher amount of functionalized single-walled carbon nanotubes a darker color was noticed, confirming that the carbon nanotubes were well dispersed.

At the macroscopic scale, grayer films were obtained by increasing functionalized single-walled carbon nanotube concentration which was the same effect visualized in the film-forming solutions. In addition, all of them were homogeneous, indicating that the solvent evaporation technique is a suitable procedure to prepare those nanocomposites. The polymer and nanofiller components interact through hydrogen bonding between protonated amino groups of chitosan and carboxylic groups found in the functionalized single-walled carbon nanotube walls and the energy involved in that is about -120 kcal mol^{-1} as described by molecular simulations [14, 19].

Scanning electron microscopy (SEM) is extensively used to analyze the morphology of polymeric materials, like surface characteristics and filler dispersion. The microstructure of films mainly depends on the interaction between the components. Scanning electron micrographs revealed that the surface of the control chitosan film (CHI) showed a smooth and homogeneous appearance at 1000 × magnification, *Figure 1*a. A homogeneous appearance for the CHCN10 film was observed that means a uniform distribution of the nanofillers was achieved in the nanocomposite films, Figure 1b. The particles with nanodimension can be, however, invisible due to the limited resolution of the scanning electron microscopy. In general, the microstructure of the films indicated appropriate compatibility between the components. All compositions containing functionalized single-walled carbon nanotubes showed similar behavior.

Uniform dispersion of nanofillers at polymer host is crucial to enhance mechanical and physical properties not found in conventional composites. To maximize the reinforcement effect, carbon nanotubes must be well dispersed to produce a large interfacial area at the nanoscale phase dimension between polymer and nanofiller. In addition, the functionalization of nanofiller is used to alter these interfacial states which directly reflects on nanofiller dispersion gain. Surface, thermal and mechanical properties were evaluated as a function of functionalized single-walled carbon nanotube concentration.

The films presented microscopic thickness and the inclusion of larger amounts of functionalized

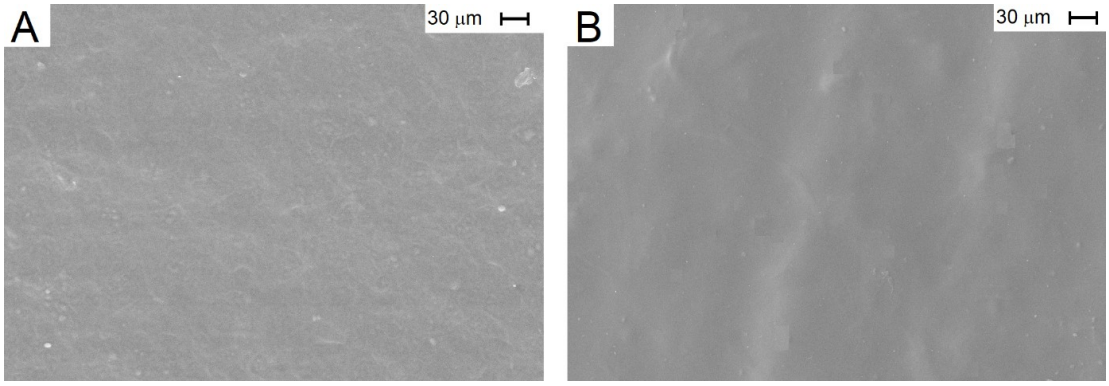

Figure 1. SEM images of (A) CHI and (B) CHCN10 films surface (magnification of 1000 x).

single-walled carbon nanotubes resulted in significantly thinner samples, as observed for CHCN25 and CHCN50, *Table 1*. The interactions between polymeric matrix and nanofillers may promote better compaction of the structure of the films, resulting in the observed effect.

Table 1. Average thickness of chitosan and chitosan/functionalized single-walled carbon nanotubes films.

Film	Average thickness (mm)
CHI	0.058 ± 0.004^{a}
CHCN10	$0.054 \pm 0.005^{a,b}$
CHCN25	0.050 ± 0.005^{b}
CHCN50	0.052 ± 0.004^{b}

Values with the same superscript letter (a-b) were not significantly different ($p > 0.05$).

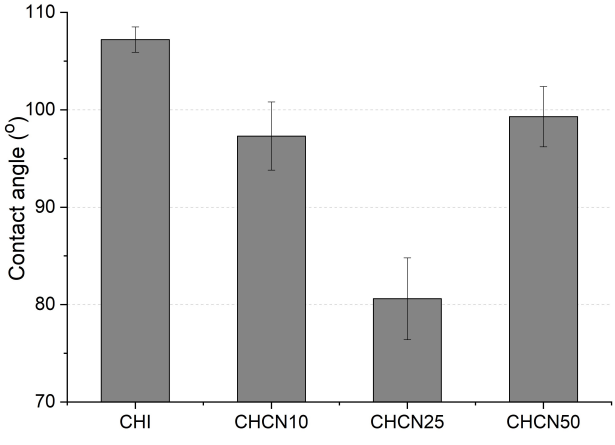

Figure 2. Contact angle values for the chitosan and nanocomposite films.

A specific contact angle is observed when a drop of solvent is placed on the film surface. The solvent does not spread, and this specific angle is a measure of the non-covalent forces between the solvent and the film's surface. The addition of functionalized single-walled carbon nanotubes decreased the contact angle values, which indicates a modification in the surface wettability of nanocomposite films, *Figure 2*.

Nanocomposite films showed more hydrophilic characteristics in comparison with the control film (CHI) although was not observed a linear increase in water affinity regarding the functionalized single-walled carbon nanotubes concentration. The influence of the nanofiller on the wettability of polymer nanocomposites can be explained by the presence of functional groups formed by the acid treatment, even though the roughness of the films should also influence this property [20].

Despite the influence of polar groups of functionalized single-walled carbon nanotubes on the hydrophilicity of the films, the increase in the nanofiller concentration can promote its aggregation, which implies a lower gain of wettability of CHCN50 in comparison with the other nanocomposite films. A similar aggregation effect was reported for multi walled carbon nanotubes/chitosan nanocomposites films, with a decrease in the mechanical properties as a function of the increase in multi walled carbon nanotube concentration [15]. Therefore, among the different functionalized single-walled carbon nanotubes concentrations analyzed, the 0.25 % (w/w) showed the minor contact angle value, $80.6 \pm 4.2°$, indicating the achievement of the hydrophilic film since contact angles smaller than 90° characterize a hydrophilic surface.

Fourier-transform infrared spectra of functionalized single-walled carbon nanotubes, chitosan and nanocomposite films confirmed the functionalization of the nanofiller and the conservation of chitosan structure after incorporation of single-walled carbon nanotubes into the polymeric matrix, *Figure 3*. functionalized single-walled carbon nanotubes spectra showed low intensity bands at 1719 and 3300 cm^{-1}, respectively, related to the carboxyl and hydroxyl groups, which evidence the effective functionalization of single-walled carbon nanotubes, while the band at 1575 cm^{-1} is related to the aromatic C=C bond stretching [21], Figure 3a. The chitosan spectrum showed the absorption bands characteristics of amides I and II at 1655 and 1560 cm^{-1}, respectively; –C–H banding at 1409 cm^{-1}; C–O and C–O–C stretching vibrations at 1153, 1094 and 1026 cm^{-1}, corresponding to the saccharide structure of chitosan; and O–H stretching at 3350 cm^{-1}, Figure 3b.

The spectra for the nanocomposite films exhibited the same vibration bands of chitosan control film, Figure 3c, d, e. This behavior can be explained by the small concentration (maximum 0.5 % w/w) and the low intensity of functionalized single-walled carbon nanotubes bands, which leads to an overlapping of the bands. The absence of shifts after the inclusion of carbon nanotubes indicated an electrostatic interaction between chitosan and the nanofiller as observed in a previous study [16]. Furthermore, no shifts in fourier-transform infrared spectroscopy bands Page 11, lines after multi walled carbon nanotube addition are described, which agrees with our study [2].

Thermal decomposition of functionalized single-walled carbon nanotubes and nanocomposite films was assessed by the analysis of thermogravimetric curves (TG) acquired in synthetic air from 25 °C to 800 °C, *Figure 4*. The purity of functionalized single-walled carbon nanotubes was qualitatively confirmed by the small residual material found at 700 °C (less than 1 %) which indicated an efficient removal of the metal catalysts on the purification step in the carbon nanotube production.

The first stage of mass loss for chitosan films (25 °C to 200 °C) is due to the loss of water, the second one (200 °C to 400 °C) refers to the polysaccharide decomposition and the third stage (500 °C to 700 °C) to the carbonization of the polymer. For the nanocomposite films the weight loss was observed in four stages: the first, between 25 °C and 110 °C, is related to the loss of hydration water, the second one (110 °C to 210 °C) is due to the loss of non-bonded linked water, the third one (210 °C to 400 °C) to the polysaccharide decomposition and the fourth stage (above 400 °C), similarly to CHI, refers to the polymer carbonization [16].

The T_{onset} and temperatures at 10 %, 25 %, 50 % and 75 % weight loss of films ($T_{10\%}$, $T_{25\%}$, $T_{50\%}$ and $T_{75\%}$) were determined using the thermogravimetric

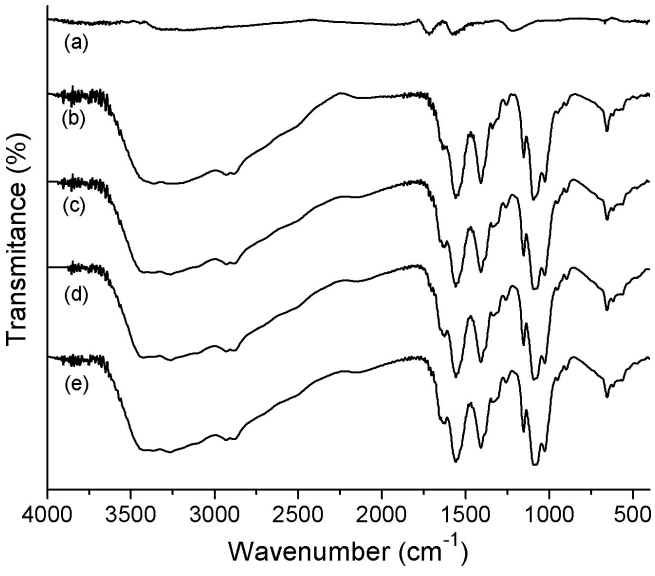

Figure 3. Fourier-transform infrared spectroscopy spectra of (a) *f*-SWCN, (b) CHI, (c) CHCN10, (d) CHCN25 and (e) CHCN50.

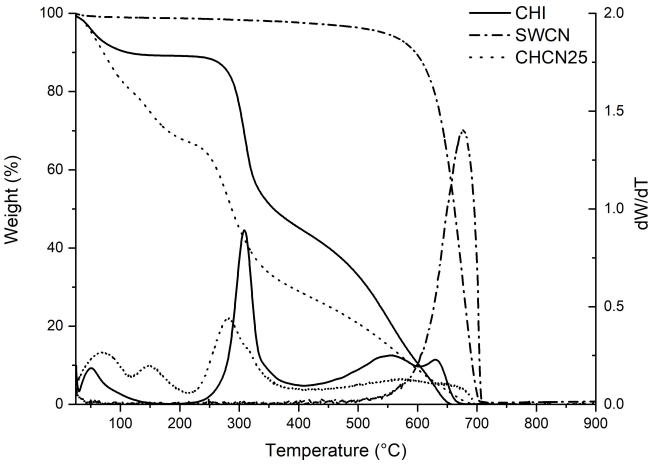

Figure 4. Typical TG/DTG curves of *f*-SWCN, CHI and CHCN25 films in synthetic air atmosphere (90 mL min^{-1}) at 10 °C min^{-1}.

curves, *Table 2*. The onset temperature denotes the temperature at which the analyzed material starts its degradation, and this is a reproducible method to determine the thermal stability of materials. Furthermore, it is a recommended method described by ASTM standards. For all samples T_{onset} was determined by the intercept of extrapolated curves in the range of the thermal event.

Values of $T_{10\%}$, $T_{25\%}$, $T_{50\%}$ and $T_{75\%}$ for the nanocomposite films show a decrease in comparison with chitosan film. Although functionalized single-walled carbon nanotubes has high thermal stability, its presence in nanocomposites does not provide an increase in thermal stability.

Despite the high thermal stability of functionalized single-walled carbon nanotubes (T_{onset} of 590 °C), its inclusion in chitosan matrix (T_{onset} of 276.4 °C) led to a decrease in the initial temperature of degradation of the films, indicated by the reduction on the T_{onset} values (250.8 °C, 253.4 °C and 256.7 °C for CHCN10, CHCN25 and CHCN50, respectively), in agreement with previously reported results [22]. An increase in functionalized single-walled carbon nanotubes concentration implied an increase in thermal stability of the nanocomposites. The presence of the nanofiller must diminish the growth of crystalline phases on the chitosan matrix since chitosan/single-walled carbon nanotubes interactions involve the amino groups of chitosan, which is crucial in the crystal growth process [23]. However, the increase of functionalized single-walled carbon nanotubes concentration resulted in a rise of thermal stability of the nanocomposite films what indicates that despite the probable crystallinity reduction due to functionalized single-walled carbon nanotubes inclusion, that tends to decrease the thermal stability of the films, the nanofiller can act as an insulator, barring the release of volatile products at the polymer degradation.

Stress-strain curves for CHI and chitosan/single-walled carbon nanotubes nanocomposite films obtained by dynamic mechanical analysis (DMA) are presented in *Figure 5*. Comparing to the control film CHI, the tensile strength at break of the nanocomposite films increased with the loading of functionalized single-walled carbon nanotubes in the polymeric matrix.

The effect of functionalized single-walled carbon nanotubes addition in the arising of mechanical properties must be related to the interactions between chitosan and the carbon nanotubes. For polymeric composites, their mechanical properties are affected by filler concentration, distribution and orientation since these parameters determine the

Table 2. T_{onset} and temperatures at 10 %, 25 %, 50 % and 75 % weight loss of films obtained by TG measurements.

Sample	T (°C)				T_{onset} (°C)
	$T_{10\%}$	$T_{25\%}$	$T_{50\%}$	$T_{75\%}$	
CHI	111.4	301.8	358.5	537.7	276.4
f-SWCN	596.6	636.5	662.1	680.6	590.0
CHCN10	72.6	154.7	290.5	465.8	250.8
CHCN25	71.1	149.0	287.2	450.8	253.4
CHCN50	68.2	150.1	292.0	451.0	256.7

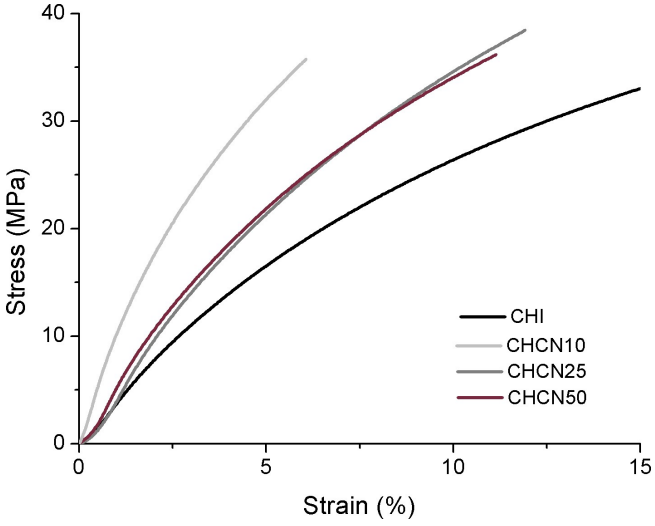

Figure 5. Stress-strain curves for chitosan and nanocomposite films.

Table 3. Elongation at break, tensile strength at break and Young's modulus for the control and nanocomposite films.

	CHI	CHCN10	CHCN25	CHCN50
Tensile strength at break (MPa)	32.52 ± 0.67^{b}	$35.03 \pm 2.42^{a,b}$	38.25 ± 0.36^{a}	36.21 ± 1.07^{a}
Elongation at break (%)	13.44 ± 1.90^{a}	6.53 ± 0.54^{b}	$11.52 \pm 2.13^{a,b}$	$10.04 \pm 3.43^{a,b}$
Young's modulus (MPa)	0.21 ± 0.07^{b}	0.54 ± 0.04^{a}	0.34 ± 0.07^{b}	0.30 ± 0.03^{b}

In the same line, values with the same superscript letter (a-b) were not significantly different ($p > 0.05$).

stress transfer from the polymeric matrix to the filler. Previous studies using multi walled carbon nanotubes indicated that the aggregation of carbon nanotubes is the limiting factor to the mechanical properties improvement since this phenomenon can facilitate arise of nanocracks at the structure of the films [6, 7].

Significant differences in the values of tensile strength at the break for the films were noted for the samples CHCN25 and CHCN50, with increases of 17.6 and 11.3 %, respectively, *Table 3*. Elongation at break of the nanocomposite films slightly decreased overall compared with CHI sample, which is a typical pattern of brittle material, despite the non-linear relationship of these properties with the functionalized single-walled carbon nanotube concentration. However, only for the CHCN10 sample, was verified a significant difference, with a reduction of 51.4 % on its value. Notably, the sample CHCN25 showed a greater increase in breaking stress values with a smaller reduction on the elongation at break values (14.3 %). The reason for the rigidity observed for the nanocomposites must be the intrinsic hardness of the carbon and its derivatives [6].

Due to its extraordinary mechanical properties, functionalized single-walled carbon nanotubes inclusion improves the properties described for the nanocomposite films, Table 3. Furthermore, Young's modulus values confirmed the enhancement of stiffness in single-walled carbon nanotubes/chitosan films. As observed before, there is no correlation between the mechanical properties values and carbon nanotube concentration which evidences a limit of saturation in the dispersion of fillers in the polymeric matrix when this preparation method was used.

Even the homogeneity of film forming solutions appearance, the properties of the nanocomposite films produced by solvent evaporation technique showed typical behavior of materials with aggregates. During the process of solvent removal, the formation of these aggregates can be observed [24]. Based on the results, like a decrease in contact angle values and mechanical properties as a function of the increase of single-walled carbon nanotubes concentration, it is possible that for higher functionalized single-walled carbon nanotubes concentrations the film has been formed with high heterogeneity. Therefore, there is a limit of functionalized single-walled carbon nanotubes that can be dispersed in the polymeric matrix by this procedure. Alternatively, a faster drying process can limit the aggregation effects.

4 Conclusion

Nanocomposite films were successfully prepared using the self-assembly association between chitosan and functionalized single-walled carbon nanotubes. A good dispersion of the nanofillers in an aqueous solution was achieved by the electrostatic interaction at lower concentrations of functionalized single-walled carbon nanotubes. The improvement in tensile strength at break property was observed by stress-strain curves, in agreement with the expected behavior of polymeric matrix reinforced with nanofillers. Furthermore, a rise in the hydrophilicity and a decrease in thermal stability after the functionalized single-walled carbon nanotubes addition was noticed. However, there is a limit of functionalized single-walled carbon nanotubes that can be dispersed in the polymeric matrix when the self-assembly method is used. For high carbon nanotubes concentrations, the arising of aggregates during the drying process can explain the unexpected characteristics.

Acknowledgements

This study was financed in part by the Coordenação de Aperfeiçoamento de Pessoal de Nível Superior - Brasil (CAPES) - Finance Code 001. M.A.V.R. and M.M.H. thank Prof. Benedito dos Santos Lima Neto for the supplied SWCN, 7 Dr. Rodrigo C. Sabadini for TG measurements and FAPESP (grant number 2010/19417-0) under responsibility of Prof. Agnieszka Pawlicka. To Christoph Morscher for help in German translation. Open access funding enabled and organized by Projekt DEAL.

5 References

[1] S.F. Wang, L. Shen, Y.J. Tong, L. Chen, I.Y. Phang, P.Q. Lim, T.X. Liu, *Polym. Degrad. Stab.* **2005**, *90*, 123.
[2] K.Y. Castrejón-Parga, H. Camacho-Montes, C.A. Rodríguez-González, C. Velasco-Santos, A.L. Martínez-Hernández, D. Bueno-Jaquez, J.L. Rivera-Armenta, C.R. Ambrosio, C.C. Conzalez, M.E. Mendoza-Duarte, P.E. García-Casillas, *J. Alloys Compd.* **2014**, *615*, S505.
[3] S. Islam, M.A.R. Bhuiyan, M.N. Islam, *J Polym. Environ.* **2017**, *25*, 854.
[4] G. Cavallaro, S. Micciulla, L. Chiappisi, G. Lazzara, *J. Mater. Chem. B* **2021**, *9*, 594.
[5] K. Pieklarz, M. Tylman, Z. Modrzejewska, *Mini-Rev Med. Chem.* **2020**, *20*, 1619.
[6] A. Aryaei, A.H. Jayatissa, A.C. Jayasuriya, *J Biomed. Mater. Res.* **2014**, *102*, 2704.
[7] S.-F. Wang, L. Shen, W.-D. Zhang, Y.-J. Tong, *Biomacromolecules* **2005**, *6*, 3067.
[8] E. Ruiz-Hitzky, P. Aranda, M. Darder, G. Rytwo, *J Mater. Chem.* **2010**, *20*, 9306.
[9] V. Bertolino, G. Cavallaro, S. Milioto, G. Lazzara, *Carbohyd. Polym.* **2020**, *245*, 116502.
[10] J.W. Rhim, *Carbohyd. Polym.* **2011**, *86*, 691.
[11] J. Šefčovičová, J. Tkac, *Chem. Pap.* **2015**, *69*.
[12] A. Kassem, G.M. Ayoub, L. Malaeb, *Sci. Total Environ.* **2019**, *668*, 566.
[13] J. Chen, L. Yan, W. Song, D. Xu, *Compos. Part A: Appl. Sci. Manuf.* **2018**, *114*, 149.
[14] D. Aztatzi-Pluma, E.O. Castrejón-González, A. Almendarez-Camarillo, J.F.J. Alvarado, Y. Durán-Morales, *J. Phys. Chem. C* **2016**, *120*, 2371.
[15] A. Kroustalli, A.E. Zisimopoulou, S. Koch, L. Rongen, D. Deligianni, S. Diamantouros, G. Athanassiou, M. Kokozidou, D. Mavrilas, S. Jockenhoevel, *J. Mater. Sci.: Mater. Med.* **2013**, *24*, 2889.
[16] M.M. Horn, V.C.A. Martins, A.M.G. Plepis, *Int. J. Biol. Macromol.* **2015**, *80*, 225.
[17] M. Rinaudo, M. Milas, P. Le Dung, *Int. J. Biol. Macromol.* **1993**, *15*, 281.
[18] L. Raymond, F.G. Morin, R.H. Marchessault, *Carbohyd. Res.* **1993**, *246*, 331.
[19] J. Venkatesan, Z.-J. Qian, B. Ryu, N. Ashok Kumar, S.-K. Kim, *Carbohyd. Polym.* **2011**, *83*, 569.
[20] S. Kim, A.A. Kafi, E. Bafekpour, Y.-I. Lee, B. Fox, M. Hussain, Y.-H. Choa, *J. Nanomater.* **2015**, *2015*, 1.
[21] H. Mahmoodian, O. Moradi, *Polym. Compos.* **2014**, *35*, 495.
[22] M. Zhang, A. Smith, W. Gorski, *Anal. Chem.* **2004**, *76*, 5045.
[23] T.S. Trung, W.W. Thein-Han, N.T. Qui, C.-H. Ng, W.F. Stevens, *Bioresource Technol.* **2006**, *97*, 659.
[24] J.P.F. Lagerwall, C. Schütz, M. Salajkova, J. Noh, J. Hyun Park, G. Scalia, L. Bergström, *NPG Asia Mater.* **2014**, *6*, e80.

Received in final form: February 19th 2021

